Electronic minibands in complex basis superlattices: a numerically stable calculation

2007 J. Phys.: Condens. Matter 19 266007

(http://iopscience.iop.org/0953-8984/19/26/266007)

IOP PUBLISHING JOURNAL OF PHYSICS: CONDENSED MATTER

J. Phys.: Condens. Matter **19** (2007) 266007 (8pp) doi:10.1088/0953-8984/19/26/266007

Electronic minibands in complex basis superlattices: a numerically stable calculation

W J Hsueh, J C Lin and H C Chen

Department of Engineering Science, National Taiwan University, 1, Section 4, Roosevelt Road, Taipei 10660, Taiwan

E-mail: hsuehwj@ntu.edu.tw

Received 14 April 2007, in final form 30 May 2007
Published 15 June 2007
Online at stacks.iop.org/JPhysCM/19/266007

Abstract

A numerically stable method for accurately determining the energy minibands of superlattices with arbitrary numbers of layers per cell is presented. Using a graph model with tangent and secant functions, we derive a set of concise and closed-form miniband edge equations for determining the miniband structure using topology theory. With the present method, it is not necessary to calculate the cosine of the Bloch phase, which may show a numerical overflow in calculation. Numerical results show that use of the miniband edge equations has better numerical stability than traditional methods in calculating the minibands of complex basis superlattices.

1. Introduction

Superlattices and multiple quantum wells have been extensively researched as novel materials for various applications in microelectronics. Determination of the miniband structures on the basis of Bloch waves is fundamental for studying the properties of electron behaviour in infinite superlattices [1]. Moreover, the minibands are also the dominant reference for semi-infinite [2–4] and finite superlattices [5–7]. Minibands of a superlattice are usually determined by solving the dispersion equation, which is obtained from the eigenvector–eigenvalue problem or the determinant of the system. For a binary superlattice, the dispersion relation has been expressed using the Kronig–Penney equation. In recent years, superlattices with a complex basis have received great interest [8–18]. When the number of layers in each cell is greater than two, the analytical expression of the dispersion relation becomes complex [11–13]. Thus, the electronic minibands for the complex basis superlattice are usually calculated by numerical methods [17–22].

The transfer matrix method [17–19] is one of the most popular methods for applying to the analysis of the complex basis superlattice. One of the advantages is that the dispersion relation for the minibands can be easily framed in a concise form, in which the cosine of the Bloch phase is expressed as half the trace of the global transfer matrix for a cell. However, the transfer matrix

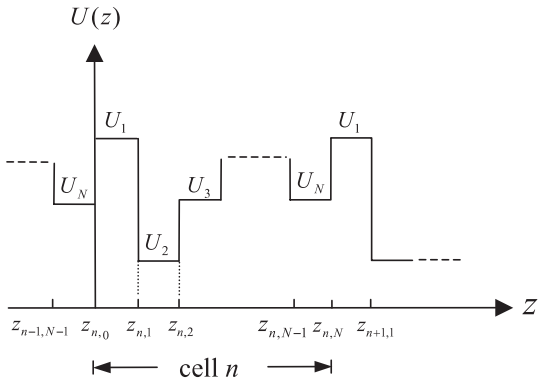

Figure 1. Potential profile of cell n of a one-dimensional complex basis superlattice with N layers per period.

method has a numerical instability problem when calculating the global transfer matrix. Some techniques have been proposed to avoid the numerical problem in computing [23]. Besides, the cosine of the Bloch phase is usually applied to determine the minibands in most numerical methods. Unfortunately, numerical instability may occur in calculating the cosine of the Bloch phase. Recently, an alternative dispersion relation expressed using tangents and cotangents was proposed to avoid the numerical problem [24]. However, calculating the minibands by the method is tedious, since the dispersion relation is gained by zeroing the determinant of a $2N \times 2N$ matrix for an N-basis superlattice.

In this paper, a two-way graph model expressed using tangent and secant functions is presented for the analysis of the electron motion in multilayer superlattices. Using the graph model and the properties of the Bloch wave, a numerically stable method for determining the minibands for complex basis superlattices is proposed. A novel miniband edge equation is derived and used to calculate the minibands rather than using the cosine of the Bloch phase. Also, each term of the equation is expressed in a concise analytical form using a topology scheme [25, 26]. Using these derived formulae, it is convenient to obtain the bandgaps of the superlattice. Besides, this method does not suffer from problems of numerical instability in solving for the minibands. As far as we know, an analytical miniband edge equation with a graph model has rarely been proposed for solving for the minibands of a general superlattice.

In section 2 the relationships of the wavefunctions in each layer of the superlattice are drawn up using a graph representation. According to the special graph model and Floquet's theorem, a concise miniband edge equation for the miniband calculation is derived. A topology theory is applied to calculate each term of the miniband edge equation without using iterative calculation. In section 3, a binary superlattice is explored to show our derived formulae. Finally an N-layer basis superlattice is examined using the proposed method and the transfer matrix method to prove the feasibility and benefits of this method.

2. The model and method

We consider an infinite superlattice with periodic cells, each of which consists of N layers as shown in figure 1. On the basis of an envelope-function approximation, the motion of an electron near the conduction band bottom is described by an effective mass equation

$$\frac{-\hbar^2}{2}\frac{\mathrm{d}}{\mathrm{d}z}\left[\frac{1}{m^*(z)}\frac{\mathrm{d}}{\mathrm{d}z}\psi(z)\right] + U(z)\psi(z) = E\psi(z), \tag{1}$$

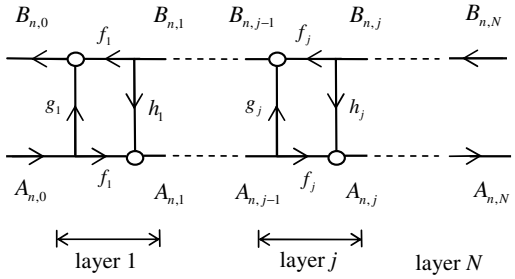

Figure 2. Graph model for cell n of a superlattice with N layers per period.

where m^* is the effective mass of the electron, $U(z)$ is the potential, and E is the electronic state energy; $\psi(z)$ is the electron wavefunction. For the structure of the superlattice, the potential barrier heights, effective mass values and thicknesses for layer j in each cell are U_j, m_j^*, and d_j, respectively. The general solution to equation (1) in the jth layer of cell n is given by

$$\psi(n, j, z) = a_{n,j}\mathrm{e}^{\mathrm{i}k_j(z-z_{n,j-1})} + b_{n,j}\mathrm{e}^{-\mathrm{i}k_j(z-z_{n,j-1})}, \tag{2}$$

where $a_{n,j}$ and $b_{n,j}$ are the amplitudes of the forward and the backward waves for the wavefunction, respectively, and k_j represent the wavevectors, $k_j = \hbar^{-1}(2m_j^*(E - U_j))^{1/2}$. The amplitudes of the forward and the backward waves of the layer can be expressed using the wavefunction at the left and the right boundaries

$$a_{n,j} = \frac{\psi(n, j, z_{n,j}) - \psi(n, j, z_{n,j-1})\,\mathrm{e}^{-\mathrm{i}k_j d_j}}{2\mathrm{i}\sin(k_j d_j)}, \tag{3a}$$

$$b_{n,j} = \frac{\psi(n, j, z_{n,j-1})\,\mathrm{e}^{\mathrm{i}k_j d_j} - \psi(n, j, z_{n,j})}{2\mathrm{i}\sin(k_j d_j)}. \tag{3b}$$

From equation (2), we have the slope of the wavefunction within layer j, $\psi'(n, j, z)$:

$$\psi'(n, j, z) = \mathrm{i}k_j(a_{n,j}\mathrm{e}^{\mathrm{i}k_j(z-z_{n,j-1})} - b_{n,j}\mathrm{e}^{-\mathrm{i}k_j(z-z_{n,j-1})}). \tag{4}$$

Substituting equations (3*a*) and (3*b*) into equations (2) and (4), the wavefunction and its slope within the layer are represented by the wavefunctions at the boundary of the layer. Using Bastard's boundary conditions, the wavefunctions at the intersection of two neighbouring layers satisfy

$$\psi(n, j, z_{n,j}) = \psi(n, j+1, z_{n,j}), \qquad \text{for } j = 1, 2, \ldots, N \tag{5a}$$

$$\frac{1}{m_j^*}\psi'(n, j, z_{n,j}) = \frac{1}{m_{j+1}^*}\psi'(n, j+1, z_{n,j}), \qquad \text{for } j = 1, 2, \ldots, N \tag{5b}$$

where layer $N+1$ of cell n is the renamed layer 1 of cell $n+1$. These relations of wavefunctions at the boundary of layer j can be described by

$$A_{n,j} = f_j A_{n,j-1} + h_j B_{n,j}, \tag{6a}$$

$$B_{n,j-1} = f_j B_{n,j} + g_j A_{n,j-1}, \tag{6b}$$

where $f_j = \sec k_j d_j$, $g_j = (k_j/m_j^*)\tan k_j d_j$, $h_j = (m_j^*/k_j)\tan k_j d_j$, $A_{n,j} = \psi(n, j, z_{n,j})$ and $B_{n,j} = \psi'(n, j, z_{n,j})/m_j^*$. Since the values of $\sec k_j d_j$, $(k_j/m_j^*)\tan k_j d_j$, and $(m_j^*/k_j)\tan k_j d_j$ do not change for either the positive or negative sign for the square root of k_j, both signs for the square root of k_j are acceptable for equations (6*a*) and (6*b*).

We can depict the relations of the amplitudes using a two-way graph model as shown in figure 2. For the model, the lower side state flows at both ends are all in the rightward flow

direction and the upper side state flows are in the leftward flow direction. Figure 2 shows the connection of the graph models for N layers in a cell of the superlattice. We see the amplitudes $A_{n,N}$ and $B_{n,0}$ are dependent on the amplitudes $A_{n,0}$ and $B_{n,N}$. Thus, $A_{n,N}$ and $B_{n,0}$ are expressed as

$$A_{n,N} = A_{n,0} f + B_{n,N} h, \tag{7a}$$

$$B_{n,0} = B_{n,N} f + A_{n,0} g. \tag{7b}$$

Since cells n and $n+1$ are connected for $n = 1, 2, \ldots$, we have $z_{n,N} = z_{n+1,0}$, $A_{n,N} = A_{n+1,0}$, and $B_{n,N} = B_{n+1,0}$.

We see that the coefficients of equations (7*a*) and (7*b*), f, g and h, are dependent on the structure of a cell of the superlattice. On the basis of the graph representation for a cell of the structure, these functions are easily calculated by a topology method. Using the topology theory [25, 26], the ratio of an output to an input for a given graph model is equal to $\sum_j P_j D_j / D$, where P_j is the path gain of the forward path j, D_j is the cofactor of the jth forward path, and D is the determinant of the graph defined by $D = 1 - \sum$ (all individual loop gains) $+ \sum$ (gain products of all possible pairs of loops that do not touch) $- \sum$ (gain products of all possible triplets of loops that do not touch) $+ \cdots$. For a cell with an N-layer basis superlattice, we see that the arrangement of the graph model for the cell shown in figure 2 is a special lead structure. Let $L_{p,q}$ be the gain of the loop passing through the downward vertical path for the pth layer and the upward vertical path for the qth layer given by

$$L_{p,q} = h_p g_q \prod_{j=p}^{q} f_j^2. \tag{8}$$

Using the topology formula, the determinant of a part of the graph model for the structure from layers p to q is represented by

$$S^{p,q} = \sum_{s=0}^{q-p} \sum_{i_{2s}=p+s}^{q} \sum_{i_{2s-1}=p+s-1}^{i_{2s}-1} \sum_{i_{2s-1}=p+s-1}^{i_{2s-1}} \sum_{i_{2s-2}=p+s-2}^{i_{2s-1}-1} \cdots \sum_{i_2=p+1}^{i_3} \sum_{i_1=p}^{i_2-1} \prod_{u=1}^{s} (-L_{i_{2u-1},i_{2u}}). \tag{9}$$

According to equation (7*a*), the function f is equal to the response of the amplitude $A_{n,N}$ related to input $A_{n,0}$ for zero $B_{n,N}$. There is only one forward path from $A_{n,0}$ to $A_{n,N}$ with gain $\prod_{j=1}^{N} f_j$. The cofactor of this forward path is equal to 1 since all of the loops contact the forward path. Thus the function f is expressed by the form

$$f = \prod_{j=1}^{N} f_j / S^{1,N}. \tag{10}$$

Equation (7*b*) shows that the function g is equal to the response of the amplitude $B_{n,0}$ related to input $A_{n,0}$ for zero $B_{n,N}$. We see there are N forward paths from $A_{n,0}$ to $B_{n,0}$. For the path passing the vertical upward path g_p, the forward path gain is $g_p \prod_{j=1}^{p-1} f_j^2$ and the cofactor is $S^{p,N}$. By the topology theory, we have

$$g = \frac{1}{S^{1,N}} \sum_{p=1}^{N} S^{p,N} g_p \prod_{j=1}^{p-1} f_j^2. \tag{11}$$

The function h given in equation (7*a*) is equal to the response of the amplitude $A_{n,N}$ related to input $B_{n,N}$ for zero $A_{n,0}$. In the same way, we can derive the function h as

$$h = \frac{1}{S^{1,N}} \sum_{p=1}^{N} S^{1,p} h_p \prod_{j=p+1}^{N} f_j^2. \tag{12}$$

According to Floquet's theorem, the wavefunction in an infinite periodic superlattice must obey the Bloch wave relations. The relations between the amplitudes at the ends of a cell are satisfied by the conditions

$$B_{n,N} = B_{n,0}\exp(\mathrm{i}KL), \tag{13a}$$

$$A_{n,0} = A_{n,N}\exp(-\mathrm{i}KL). \tag{13b}$$

Substituting equations (13*b*) and (13*a*) into equations (7*a*) and (7*b*) yields

$$1 - gh + f^2 - 2f\cos(KL) = 0. \tag{14}$$

The forbidden gap is given by the condition of $|\cos(KL)| > 1$. With this condition, the Bloch wavenumber K is complex and the Bloch wave is evanescent. The allowed energy band occurs when $|\cos(KL)| \leqslant 1$. In the allowed energy band, K is a real value and the Bloch wave is propagating in the superlattice. The kernel of calculating miniband structure is finding the band edge, which occurs for the condition $\cos(KL) = \pm 1$. By substituting $\cos(KL) = \pm 1$ into equation (14), we have the miniband edge equations

$$(1 \mp f)^2 - gh = 0. \tag{15}$$

Equations (15) are the major equations of this paper. Using equations (15), it is not required to calculate $\cos(KL)$ in finding the miniband edge. Also, the centre of allowed minibands, using $\cos(KL) = 0$, can be written as

$$1 - gh + f^2 = 0. \tag{16}$$

The miniband centre equation given in equation (16) can be used to check the regime for the allowed minibands.

In most numerical methods, $\cos(KL)$ is used to determine the miniband structure. First, the values of $\cos(KL)$ related to energy higher than the minimum value of U_j are calculated. Next, the band edges are determined using the condition $\cos(KL) = \pm 1$. However, calculation of $\cos(KL)$ may have numerical overflow as shown in the following numerical examples.

3. Results and discussion

3.1. Theoretical demonstration using a binary superlattice

To demonstrate the present theory, a simple case of a two-layer based superlattice is studied since the typical dispersion equation for the simple case is well known. The potential barrier heights, effective mass values and thicknesses for layer 1 of a cell are U_a, m_a^*, and d_a, respectively, and those for layer 2 are U_b, m_b^*, and d_b. Let us consider the condition $U_a < U_b$. The wavevectors corresponding to layers 1 and 2 are $k_a = \hbar^{-1}(2m_a^*(E - U_a))^{1/2}$ and $k_b = \hbar^{-1}(2m_b^*(E - U_b))^{1/2}$ respectively. The miniband structure is first examined to verify the miniband edge equations presented as equations (15). To get the transmission and reflection coefficients, the determinant for each cell should be calculated. A detailed procedure for calculating the determinant for each cell using our method is shown as follows. For the case of $U_b < E$, both k_a and k_b are real values. According to equation (9), we have $S^{1,2} = \sum_{s=0}^{1} A_s$. Since there is no summing operation required for $s = 0$, we have $A_0 = 1$. For $s = 1$, a pair of summing operations is required, $A_1 = \sum_{n_2=2}^{2}\sum_{n_1=1}^{n_2-1}(-L_{n_1,n_2}) = -L_{1,2}$. From equation (8), $L_{1,2}$ is given by $L_{1,2} = \frac{m_a^* k_b t_a t_b}{m_b^* k_a}$, where t_j is the symbol for $\tan k_j d_j$, $j = a, b$. Thus we have $S^{1,2}$ expressed as $S^{1,2} = 1 - L_{1,2}$. According to equations (10)–(12), we have $f = e_a e_b / D$, $g = (k_a t_a / m_a^* + k_b t_b / m_b^*)/D$ and $h = (m_b^* t_a / k_a + m_a^* t_b / k_b)/D$, $D = 1 - (k_b m_a^* / k_a m_b^*) t_a t_b$,

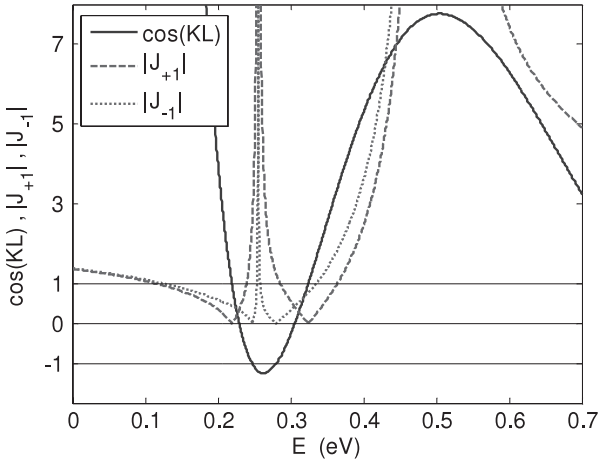

Figure 3. Comparison of $\cos(KL)$ and absolute values of $J_{\pm 1}$ for a biperiodic superlattice, in which the width of each layer is 2 nm and the concentrations in each of the layers are $x_1 = x_3 = 0$, $x_2 = 0.5$, $x_4 = 0.7$, where the subscript of x corresponds to the number of the layer.

where e_j is the symbol for $\sec k_j d_j$, $j = a, b$. Using equations (15), we can derive the miniband edge equation as

$$1 - \frac{1}{2}\left(\frac{k_a m_b^*}{k_b m_a^*} + \frac{k_b m_a^*}{k_a m_b^*}\right) t_a t_b \mp e_a e_b = 0. \tag{17}$$

For the condition $U_a < E < U_b$, k_a is real and k_b is imaginary. Thus, k_b is usually redefined as $\mathrm{i}\kappa_b$, where κ_b is a real value. Besides, $\sec(k_b d_b)$ and $\tan(k_b d_b)$ are replaced by $\mathrm{sech}(\kappa_b d_b)$ and $\mathrm{i}\tanh(\kappa_b d_b)$. In the condition, equation (17) is identical to the band edge condition from the typical dispersion equation, $\cos(KL) = \pm 1$, in traditional methods [1].

3.2. Numerical examples of multilayer superlattices

For numerical implementation of the present theory, a biperiodic (four-layer basis) superlattice made of $\mathrm{Al}_x\mathrm{Ga}_{1-x}\mathrm{As}$ is examined. The effective mass and potential of the $\mathrm{Al}_x\mathrm{Ga}_{1-x}\mathrm{As}$ layer are $m^*(x) = (0.067 + 0.083x)m_e^*$ and $U(x) = 944x$ meV, respectively. The concentration for each layer is $x_1 = x_3 = 0$, $x_2 = 0.5$, $x_4 = 0.7$, in which the subscript of x corresponds to the number of the layer. The widths of all layers are the same, equal to 2 nm. As we know, the minibands for the superlattice are usually determined by the function $\cos(KL)$ calculated using the traditional dispersion equation. However, the miniband edge equations, given as equations (15), are used in this method. Here, we define the left-hand sides of equations (15) and (16) as respectively $J_{\pm 1}$ and J_0, which are dependent on the energy E. The roots of $J_{\pm 1} = 0$ are just located at the edges of the allowed bands. The absolute values of $J_{\pm 1}$ and $\cos(KL)$ for the energy $E > 0$ were plotted for comparison, as shown in figure 3. We see that the solutions of $J_{\pm 1} = 0$ are just equal to those of $\cos(KL) = \pm 1$.

For the width of each layer varied over the range from 2 to 200 nm, the miniband analyses by the present method and traditional methods are compared. The maximum absolute values of $\cos(KL)$, used in the traditional method, and those of $J_{\pm 1}$ and J_0, used in this method, versus the width of each layer are shown in figure 4. We see that $\max(|\cos(KL)|)$ in traditional analysis increases in exponent versus the width of each layer but $\max(|J_{+1}|, |J_{-1}|, |J_0|)$ in this method do not enlarge with increasing width.

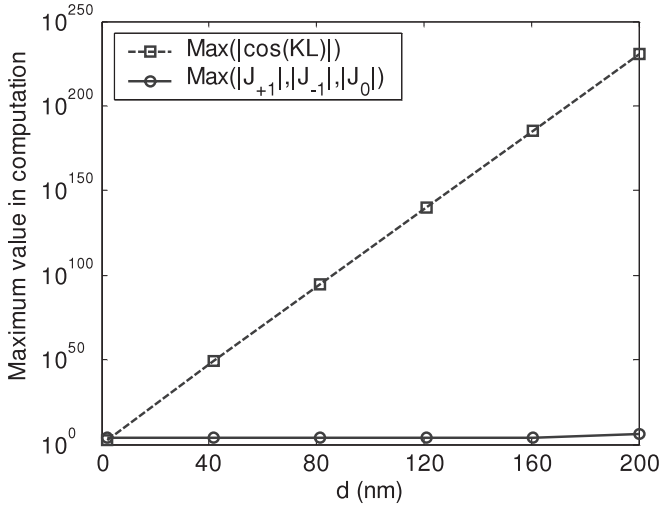

Figure 4. The maximum absolute values of $\cos(KL)$, $J_{\pm 1}$ and J_0 versus the width of each layer for a biperiodic superlattice made of $Al_xGa_{1-x}As$. The concentrations in each of the layers are $x_1 = x_3 = 0, x_2 = 0.5, x_4 = 0.7$.

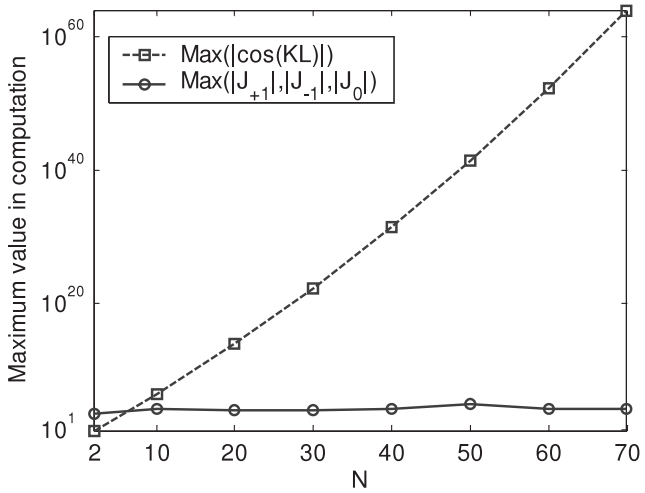

Figure 5. The maximum absolute values of $\cos(KL)$, $J_{\pm 1}$ and J_0 for an N-layer basis superlattice. The parameters are $d_n = 2(1 + \frac{n}{N})$ nm, $x_1 = x_3 = \cdots = x_{N-1} = 0$, $x_2 = x_4 = \cdots = x_N = 0.5$.

We next study the numerical implementation for an N-layer superlattice, in which the concentration of each odd layer is 0 and that of each even layer is 0.5. For each period, the width of each layer is $d_n = 2(1 + \frac{n}{N})$ nm. For calculating the miniband structures, with N is varied from 2 to 70, the absolute values of $\cos(KL)$, $J_{\pm 1}$ and J_0 versus N are shown in figure 5. We can see that $\max(|J_{+1}|, |J_{-1}|, |J_0|)$, used in this method, is almost constant but $\max(|\cos(KL)|)$, used in traditional methods, enlarges exponentially with increasing N. These results show that this method provides more robust numerical stability than traditional methods.

4. Conclusions

We have proposed a novel method for finding the miniband structure of complex basis superlattices. In this paper, we derive a set of miniband edge equations, equations (15), for computing the minibands of general basis superlattices based on a two-way graph model with tangent and secant functions. These new equations can be directly used to solve for the edge of the minigap without computing the cosine of the Bloch phase. Numerical results show that use of the equations presented to find the minibands has more stability than use of the cosine of the Bloch phase in traditional methods. Also, the coefficients of the miniband edge equation are expressed using three characteristic functions, f, g, h, for a cell of the periodic structure. Analytical and concise expressions for each characteristic function are derived and shown in equations (10)–(12). Thus, it is convenient to obtain the miniband edge equation and its coefficients from the derived formulae without recursive calculation. Although the minibands of superlattices have been examined in this paper, it is easy to extend the method and the idea of the study to more properties for infinite, semi-infinite or finite superlattices.

Acknowledgment

The author acknowledges the support in part by the National Science Council of the Republic of China under grant number NSC 94-2611-E-002-008.

References

[1] Bastard G 1988 *Wave Mechanics Applied to Semiconductor Heterostructures* (France: Les Editions de Physique)
[2] Trzeciakowski W 1988 *Phys. Rev.* B **38** 12493
[3] Bloss W L 1991 *Phys. Rev.* B **44** 8035
[4] Steslicka M, Kucharczyk R, Akjouj A, Djafari-Rouhani B, Dobrzynski L and Davison S G 2002 *Surf. Sci. Rep.* **47** 93
[5] Pereyra P 2005 *Ann. Phys.* **320** 1
[6] Sprung D W, Sigetich J D and Wu H 2000 *Am. J. Phys.* **68** 715
[7] Ren S Y 2001 *Phys. Rev.* B **64** 035322
[8] Patanè A, Sherwood D, Eaves L, Fromhold T M, Henini M, Main P C and Hill G 2002 *Appl. Phys. Lett.* **81** 661
[9] Rourke D E, Khodarinova L A and Fromhold T M 2005 *Phys. Rev.* B **72** 155334
[10] Fromhold T M, Patanè A, Bujkiewicz S, Wilkinson P B, Fowler D, Sherwood D, Stapleton S P, Krokhin A A, Eaves L, Henini M, Sankeshwar N S and Sheard F W 2004 *Nature* **428** 726
[11] Shi J J and Pan S H 1993 *Phys. Rev.* B **48** 8136
[12] Kucharczyk R, Steslicka M, Akjouj A, Djafari-Rouhani B, Dobrzynski L and El Boudouti E H 1998 *Phys. Rev.* B **58** 4589
[13] Kucharczyk R, Steslicka M and Djafari-Rouhani B 2000 *Phys. Rev.* B **62** 4549
[14] Coquelin M, Pacher C, Kast M, Strasser G and Gornik E 2006 *Phys. Status Solidi* b **14** 3692
[15] Schrottke L, Hey R and Grahn H T 1999 *Phys. Rev.* B **60** 16635
[16] Choi K K, Levine B F, Bethea C G, Walker J and Malik R J 1987 *Phys. Rev. Lett.* **59** 2459
[17] Jiang H X and Lin J Y 1986 *Phys. Rev.* B **33** 5851
[18] Yuh P F and Wang K L 1988 *Phys. Rev.* B **38** 13307
[19] Vasilopoulos P, Peeters F M and Aitelhabti D 1990 *Phys. Rev.* B **41** 10021
[20] Zarate J E and Velasco V R 2001 *Phys. Rev.* B **65** 045304
[21] Fernandez-Alvarez L, Monsivais G and Velasco V R 1996 *J. Phys.: Condens. Matter* **8** 8859
[22] Mayer A 2006 *Phys. Rev.* E **74** 046708
[23] Mayer A and Vigneron J-P 1999 *Phys. Rev.* E **59** 4659
[24] Szmulowicz F 1996 *Phys. Rev.* B **54** 11539
[25] Swamy M N S and Thulasiraman K 1981 *Graphs, Networks, and Algorithms* (New York: Wiley)
[26] Mayeda W 1972 *Graph Theory* (New York: Wiley)